EXERGY ANALYSIS OF SOLAR PHOTO VOLTAIC THERMAL HYBRID HEAT PUMP WORKING WITH CIRCULAR AND TRIANGULAR EVAPORATOR TUBE CONFIGURATIONS

N. Gunasekar[1], M. Mohanraj[2], G. Sathish Sharma[3], R. Prakash[3*]

[1]Department of Mechanical Engineering, Sri Ramakrishna Engineering College, Coimbatore,
[2] Department of Mechanical Engineering, Hindusthan College of Engineering and Technology,
Coimbatore-641032, India. [3]School of Mechanical Engineering, VIT University, Vellore campus,
Vellore- 632 014, India.   E.Mail: *drprakashvit@gmail.com

ABSTRACT

In order to evaluate the performance of a solar photovoltaic thermal hybrid heat pump working with circular and triangular tube evaporator configurations, exergy analysis is performed in this study. The experiments were carried out under the meteorological conditions of Coimbatore city (latitude of 10.98°N and longitude of 76.96°E) in India. Exergy destruction and exergy efficiency of each components of the system were calculated with reference to four ambient conditions such as solar intensity, ambient temperature, ambient relative humidity and ambient wind velocity. The exergy performance parameters of the heat pump were simulated using artificial neural networks to have accurate exergy performance comparison. The results indicated that maximum exergy destruction for both the configurations occurred in PV-T evaporator. The exergy destruction in circular tube configuration is 2-7% higher than triangular tube configuration. It was also found out that exergy efficiency of the system using triangular tube configuration is 1.2-3.8% higher than circular tube configuration.

Keywords – Photovoltaic thermal evaporators, Exergy analysis, Heat pumps

Abbreviations

Ex_{dest}	Exergy destruction (W)
$\dot{W}_{comp}$	Compressor power consumption (W)
Ex_{Qw}	Output exergy rate in the condenser (W)
$\sum \dot{I}_{rr}$	Total exergy destruction (W)
η_{mech}	Mechanical efficiency of compressor
η_{elec}	Electrical efficiency of compressor
$\dot{m}_a$	mass flow rate of air (kg/s)
$\dot{m}_r$	mass flow rate of refrigerant (kg/s)
Ac	Area of the collector (m^2)
$\dot{I}$,	collector irreversibility
$T_{o,}$	ambient temperature (K)
$T_{pl,}$	photovoltaic panel temperature (K)
T_s	Solar radiation temperature (K)
T_{sky}	Sky temperature (K).

INTRODUCTION

The photovoltaic–thermal evaporator (PV–TE) is directly integrated with the heat pump. The refrigerant flowing in the evaporator undergoes phase change from liquid to vapour by absorbing the heat from the photovoltaic panel and thereby increasing the energy conversion efficiency of PV-TE. Ji, et al., (2008) investigated the energy performance of a SPV-THP using variable frequency compressor under the meteorological conditions of Hong Kong, China and reported a maximum COP of around 10.0 and photovoltaic efficiency of about 13.4%. Shan, et al., (2014) theoretically simulated the energy performance of a PV-T hybrid collector (using R410A as a working fluid) under the meteorological conditions of Nanjing, China. Their results established that refrigerant based collectors performed better than air and water-based collectors. (Mohanraj, et al., 2016) compared the energy performance of heat pump using PV-TE with circular and triangular tube configurations using R134A as refrigerant and found that triangular tube PV–TE configuration has enhanced the major energy performance parameters of the heat pump such as, condenser heating capacity, COP and panel efficiency by 3%–7%, 3%–5% and 4%–13%, respectively when compared to the circular tube PV–TE configuration. Badescu, (2002) investigated the thermodynamic behaviour of a solar assisted heat pump and reported that maximum exergy losses occurs during compression in compressor and condensation in the condenser. Artificial Neural Network (ANN) is useful tool for performance simulation. Ceylan et al., (2008) developed an artificial neural network model for prediction of moisture content, drying air velocity and drying time in a heat pump drier. The results showed that artificial neural network predicted values were found to be closer to experimentally observed values with a correlation coefficient was 0.9999. Fannou et al., (2014) predicted the performance of ground source heat pump using artificial neural network. In their work, the compressor power consumption and condenser heating capacity were predicted with reference to

inlet and outlet evaporator pressures and evaporator temperatures, inlet temperature of condenser cold water and compressor discharge pressure. The exergy performance of the solar-assisted heat pump was predicted using ANN by Mohanraj, et al., (2010). In their study, the influence of relative humidity and wind velocity was ignored due to the presence of glazing surface over the absorber plate.

The cited literature review confirmed that there is no specific work reported on exergy analysis of SPV-THP with circular and triangular evaporator tube configuration. In this research work, the exergy performance of SPV-THP working with circular and triangular PV-TE was evaluated.

Experiments

Experimental setup: The experimental study was done in Coimbatore, India (Latitude 10.98ºN and longitude 76.96ºE). The photographic views of the fabricated SPV-THP are shown in Figure 1a and 1b. The system consists of R134a based hermetically sealed reciprocating compressor, a finned tube forced convection air cooled condenser a capillary tube expansion device and a PV–TE of an area 1.92 m^2 (1.96 m × 0.98 m) with 9.52 mm diameter circular tubes and 12 mm equilateral triangular tubes. Above absorber plate, photovoltaic panel is placed.
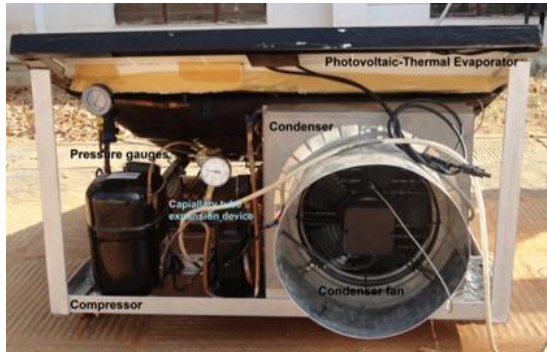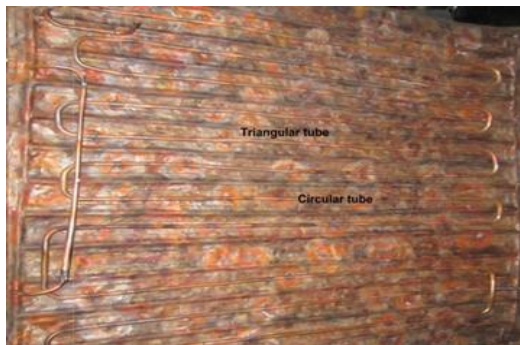

Figure 1a: Experimental Setup

Figure 1b: Absorber plate with circular and triangular tubes

The PV–TE is tilted to an angle of about 20° with respect to the horizontal and oriented towards south to maximize the solar radiation incident on the collector.

Experimental procedure: The temperature and pressure of refrigerant at typical locations in heat pump circuit, average temperature of photovoltaic panel at three different locations over the panel surface and photovoltaic output were recorded every 30 minutes. Air temperatures at entry and exit of the condenser, air flow rate through the condenser and compressor instantaneous power consumption were measured at 30-minute interval. Similarly, solar intensity, ambient temperature, ambient wind velocity and ambient relative humidity were measured at the same time interval.

Exergy analysis of heat pump: Exergy analysis method is employed to detect and to evaluate quantitatively the causes of the thermodynamic imperfection of the process under consideration. In the equations, point 1 represents the condition of refrigerant at entry of compressor, 2 represents condition at exit of compressor, 3 represents condition of refrigerant at entry of expansion valve and 4 represents condition of refrigerant at entry of PV-TE. Point 5 and 6 represents the condition of air at entry and exit of condenser respectively.

Compressor: The compressor power consumption is given by

$$\dot{W}_{comp} = \frac{\dot{m}_r (h_2 - h_1)}{\eta_{mech} \times \eta_{elec}} \qquad (1)$$

Here, $\eta_{mech} = 0.85$, $\eta_{elec} = 0.9$. The mass flow rate of the refrigerant circulated in the refrigeration system is calculated as 0.03 kg/s. The exergy destruction $\dot{Ex}_{dest(comp)}$ and exergy efficiency (ε_{comp}) of the compressor are calculated by using the following equations

$$\dot{Ex}_{dest(comp)} = \dot{Ex}_1 - \dot{Ex}_2 + \dot{W}_{comp} \qquad (2)$$

$$\varepsilon_{comp} = \frac{\dot{Ex}_2 - \dot{Ex}_1}{\dot{W}_{comp}} \qquad (3)$$

Condenser: The exergy destruction $\dot{Ex}_{dest(cond)}$ in the condenser and exergy efficiency or condenser effectiveness (ε_{cond}) are calculated by using the following equations

$$\dot{Ex}_{dest(cond)} = (\dot{Ex}_2 - \dot{Ex}_3) + (\dot{Ex}_6 - \dot{Ex}_5) \qquad (4)$$

$$\varepsilon_{cond} = \frac{\dot{m}_a (ex_6 - ex_5)}{\dot{m}_r (ex_2 - ex_3)} \qquad (5)$$

Expansion valve: The exergitic destruction ($\dot{Ex}_{dest\,(EV)}$) and exergy efficiency (ε_{EV}) are calculated by the following equations.

$$\dot{Ex}_{dest\,(EV)} = \dot{Ex}_3 - \dot{Ex}_4 \qquad (6)$$

$$\varepsilon_{EV} = 1 - \frac{\dot{Ex}_{dest}}{\dot{Ex}_{in}} \qquad (7)$$

Photovoltaic-thermal evaporator: The amount of exergy used ($\dot{Ex}_{in}$) in the system and amount of exergy collected ($\dot{Ex}_{collected}$) in the system are calculated using the following equations [9]

$$\dot{Ex}_{in} = Ac\,\dot{I}\left[1 + \frac{1}{3}\left(\frac{T_0}{T_s}\right)^4 - \frac{4}{3}\left(\frac{T_0}{T_s}\right)\right] \qquad (8)$$

$$\dot{Ex}_{out} = \dot{Ex}_{electrical} + \dot{Ex}_{thermal} \qquad (9)$$

Exergy of thermal energy ($\dot{Ex}_{thermal}$) is given by

$$\dot{Ex}_{thermal} = Q\left[1 - \frac{T_a}{T_{pl}}\right] \qquad (10)$$

The instantaneous exergy destruction ($Ex_{dest\,(SC)}$) and exergy efficiency (ε_{SC}) of solar collector can be calculated using the following equations

$$\dot{Ex}_{dest\,(SC)} = \dot{Ex}_{collected} - \dot{Ex}_{used} \qquad (11)$$

$$\varepsilon_{(SC)} = \frac{\dot{Ex}_{out}}{\dot{Ex}_{in}} \qquad (12)$$

RESULTS AND DISCUSSIONS

Exergy destruction: The results showed that maximum exergy destruction for both the configuretions occurs in PV-T evaporator followed by compressor, condenser and expansion valve, respectively. High exergy destruction for both the evaporator configurations occurs in the system during peak sunshine hours due to the fluctuations in solar radiation, heat generation in photovoltaic panels, temperature difference between absorber plate and ambient temperature, impact of ambient relative humidity and ambient wind velocity. The exergy destruction in the compressor is due to pressure ratio, energy conversion and compression effect of refrigerant in the compressor. In the condenser, exergy destruction occurs due to irreversibility associated with refrigerant properties, heat exchanger geometry, air flow rate and due to the temperature difference with the working fluids. Low exergy destruction occurs in expansion valve due to its lower irreversibility compared to other

components. The system exergy destruction for circular and triangular tube configurations of PV-T evaporators is compared in Fig. 2. The exergy destruction varies between 0.95 kW and 2.26 kW for circular tube configuration, and 0.9 kW and 2.15 kW for triangular tube configuration. The exergy destruction in circular tube configuration is 2-7% higher than triangular tube configuration.
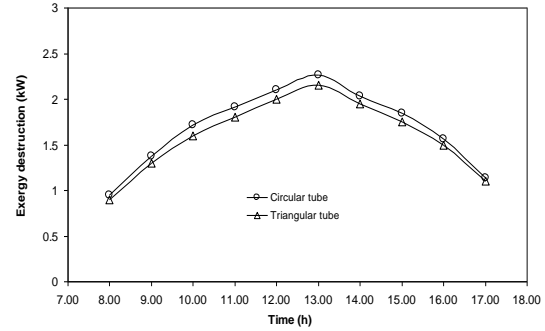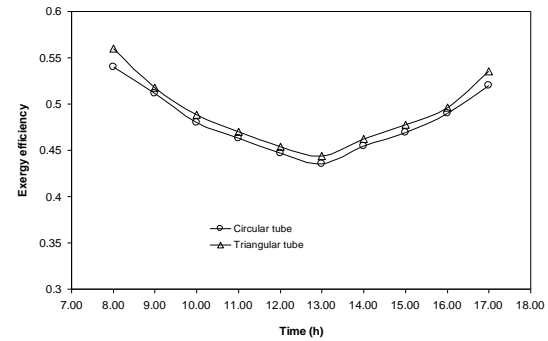

Figure 2: Variation of exergy destruction

Figure 3: Variation of exergy efficiency

Exergy efficiency: The exergy efficiency of SPV-THP system using circular and triangular tube configurations is compared in Fig.3. The exergy efficiency of SPV-THP with circular configuration varied from 0.43 to 0.54 with an average value of 0.48, whereas, the exergy efficiency of SPV-THP with triangular tube configuration varied from 0.44 to 0.56 with an average valve of 0.49. It is observed that exergy efficiency of the system using triangular tube configuration is 1.2-3.8% higher than circular tube configuration. Since the triangular tube configuration is capable of absorbing more heat compared to circular tube configuration, the irreversibility in the PV-T evaporator is reduced.

Conclusions

The maximum exergy destruction for both circular and triangular configuration SPV-THP occurred in PV-T evaporator followed by compressor, condenser and expansion valve. The exergy destruction in circular tube configuration is 2-7% higher than triangular tube configuration. The exergy efficiency of the system using triangular tube

configuration is 1.2-3.8% higher than circular tube configuration.

Scope for future work

Performance of the SPV-THP with spiral tube configurations may be tried and the effect of dust accumulation over the photovoltaic surface on the performace of SPV-THP can be studied.

REFERENCES

Badescu, V., First and second law analysis of a solar assisted heat pump- based heating system. Energy conversion and Management 43 (18): 2539-2552 (2002)

Ceylan, I. and M. Aktas, Modeling of a hazelnut dryer assisted heat pump by using artificial neural networks. Applied Energy 85(9): 841-854 (2008)

Fannou, J.L., C. Rousseau, L. Lamarche and S. Kajl, Modeling of direct expansion geothermal heat pump using artificial neural networks, Energy and Buildings 81: 381-390 (2014)

Hepbasli., A key review on exergetic analysis and assessment of renewable energy resources for a sustainable future. Renewable and Sustainable Energy Reviews 12 (3): 593-661 (2008)

Ji J., G. Pei, TT. Chow, K. Liu, H. He, J. Lu and C. Han, Experimental study of photovoltaic solar assisted heat pump system. Solar Energy 82(1): 43-52 (2008).

Kara O., K. Ulgen and A. Hepbasli, Exergitic assessment of a direct expansion solar assisted heat pump systems: Review and modelling. Renewable and Sustainable Energy Reviews 12(15): 1383-1401 (2008)

Mekhilef S., R. Saidur and M. Kamalisarvestani, Effect of dust, humidity and air velocity on efficiency of photovoltaic cells. Renewable and Sustainable Energy Reviews 16(5): 2920-2925 (2012)

Mohanraj M., N. Gunasekar and V. Velmurugan, Comparison of energy performance of heat pumps using a photovoltaic– thermal evaporator with circular and triangular tube configuretions. Building simulation 9: 27–41 (2016)

Mohanraj M., S. Jayaraj and C. Muraleedharan, Applications of artificial neural networks for refrigeration, air conditioning and heat pump systems - A review. Renewable and Sustainable Energy Reviews 16(2): 1340-1358 (2012)

Mohanraj M., S. Jayaraj and C. Muraleedharan, Exergy assessment of a direct expansion solar assisted heat pump working with R22 and R407C/LPG mixture. International Journal of Green Energy 7 (1): 65-83 (2010)

Shan F., F. Tang, L. Cao and G. Fang, Performance evaluations and applications of photovoltaic– thermal collectors and systems. Renewable and Sustainable Energy Reviews 33: 467-483 (2014)

Shariah., M.A., Al-Akhras and I.A. Al-Omari, Optimizing the tilt angle of solar collectors. Renewable Energy 26 (4): 587- 598 (2002)

Sudhakar K., and T. Srivastava, Energy and Exergy analysis of 36W solar photovoltaic module. International Journal of Ambient Energy 35(1): 51-57 (2013)